Physics Letters B 671 (2009) 10–14

Contents lists available at ScienceDirect

Physics Letters B

www.elsevier.com/locate/physletb

On prospects for dark matter indirect detection in the Constrained MSSM

Leszek Roszkowski [a,*], Roberto Ruiz de Austri [b], Joe Silk [c], Roberto Trotta [c]

[a] Department of Physics and Astronomy, University of Sheffield, Sheffield S3 7RH, UK
[b] Departamento de Física Teórica C-XI and Instituto de Física Teórica C-XVI, Universidad Autónoma de Madrid, Cantoblanco, 28049 Madrid, Spain
[c] Oxford University, Department of Astrophysics, Denys Wilkinson Building, Keble Road, Oxford, OX1 3RH, UK

ARTICLE INFO

Article history:
Received 16 June 2008
Received in revised form 1 October 2008
Accepted 13 November 2008
Available online 28 November 2008
Editor: G.F. Giudice

PACS:
12.60.Jv
14.80.Ly
95.35.+d

ABSTRACT

We apply a rigorous statistical analysis to the Constrained MSSM to derive the most probable ranges of the diffuse gamma radiation flux from the direction of the Galactic center and of the positron flux from the Galactic halo due to neutralino dark matter annihilation, for several different choices of the halo model and propagation model parameters. We find that, for a specified halo profile, and assuming flat priors, the 68% probability range of the integrated γ-ray flux spans about one order of magnitude, while the 95% probability range can be much larger and extend over four orders of magnitude (even exceeding five for a tiny region at small neutralino mass). The detectability of the signal by GLAST depending primarily on the cuspiness of the halo profile. The positron flux, on the other hand, appears to be too small to be detectable by PAMELA, unless the boost factor is at least of order ten and/or the halo profile is extremely cuspy. We also briefly discuss the sensitivity of our results to the choice of priors.

1. Introduction

There is currently much evidence for the existence of large amounts of dark matter (DM) in the Universe. While its nature remains unknown, DM is likely to be made up of an exotic species of weakly interacting massive particles (WIMPs). A particularly popular WIMP candidate is the lightest neutralino χ of effective low-energy supersymmetry (SUSY), which is stable due to R-parity [1,2]. In addition to collider searches for SUSY and direct detection (DD) searches for a cosmic WIMP, a promising strategy is that of indirect detection (ID), i.e., a search for traces of WIMP pair-annihilation in the Milky Way. Since the annihilation rate is proportional to the square of the WIMP number density, of particular interest are the Galactic center (GC) and nearby clumps in the halo where the density of DM is believed to be enhanced. The aim of this Letter is to provide, for the first time, a statistical measure for the prediction of γ-ray and positron signatures in low-energy SUSY, thus allowing one to assess high-probability regions for DM-annihilation signatures that could be observed by the GLAST (in orbit since June 2008) and PAMELA (launched 2006) satellites. Existing data from EGRET suggest a spectrally distinct excess of γ-rays up to ~ 10 GeV and the HEAT data indicate a possible excess in positron flux between 5 to ~ 30 GeV. GLAST and PAMELA will provide an order of magnitude more sensitivity.

In assessing detection prospects of WIMPs there are two main sources of uncertainties. One comes from the underlying particle physics model where WIMP mass and annihilation cross section can vary over a few orders of magnitude. The other is astrophysical in nature and stems from substantial uncertainties in the DM distribution, both locally (local DM density and the existence of clumps) and towards the GC. Since the general Minimal Supersymmetric Standard Model (MSSM) suffers from a lack of predictability due to a large number of free parameters, it is interesting and worthwhile to assess WIMP detection prospects in more constrained and more well-motivated low-energy SUSY models, among which particularly popular is the Constrained MSSM (CMSSM) [3], which includes the minimal supergravity model [4]. By applying a statistical approach, we derive in the CMSSM most probable ranges of fluxes, thus bringing under control all the uncertainties of the particle physics side of WIMP detection. This is a major improvement over existing methods which are usually limited to the consideration of a few representative choices of points or slices in the parameter space. Detection prospects then become a function of specific astrophysical uncertainties only.

In this Letter we employ a Bayesian Markov Chain Monte Carlo (MCMC) technique to efficiently explore the multi-dimensional parameter space of the CMSSM, and to include all relevant sources of uncertainty on the particle physics side [5,6] (for a similar study, see [7]). Our Bayesian approach allows us to produce probability maps for all relevant observable quantities, thus establishing a complete set of predictions of the CMSSM.

* Corresponding author.
E-mail addresses: l.roszkowski@sheffield.ac.uk (L. Roszkowski), rruiz@delta.ft.uam.es (R. Ruiz de Austri), silk@astro.ox.ac.uk (J. Silk), rxt@astro.ox.ac.uk (R. Trotta).

0370-2693
doi:10.1016/j.physletb.2008.11.061

2. Bayesian analysis of the CMSSM

The CMSSM is described in terms of four free parameters: a ratio of Higgs vacuum expectation values $\tan\beta$, and common soft SUSY-breaking mass parameters of gauginos, $m_{1/2}$, scalars, m_0, and tri-linear couplings, A_0. The parameters $m_{1/2}$, m_0 and A_0 are specified at the GUT scale, $M_{\rm GUT} \simeq 2\times 10^{16}$ GeV, which serves as a starting point for evolving the MSSM renormalization group equations for couplings and masses down to a low energy scale $M_{\rm SUSY} \equiv \sqrt{m_{\tilde{t}_1} m_{\tilde{t}_2}}$ (where $m_{\tilde{t}_1,\tilde{t}_2}$ denote the masses of the scalar partners of the top quark), chosen so as to minimize higher order loop corrections. At $M_{\rm SUSY}$ the (1-loop corrected) conditions of electroweak symmetry breaking (EWSB) are imposed. The sign of the Higgs/higgsino mass parameter μ, however, remains undetermined. Here we set $\mu > 0$.

In deriving predictions for the observable quantities, one also needs to take into account the uncertainty coming from our imperfect knowledge of the values of some relevant Standard Model (SM) parameters, namely the pole top quark mass, M_t, the bottom quark mass at m_b, $m_b(m_b)^{\overline{\rm MS}}$, and the electromagnetic and the strong coupling constants at the Z pole mass M_Z, $\alpha_{\rm em}(M_Z)^{\overline{\rm MS}}$ and $\alpha_s(M_Z)^{\overline{\rm MS}}$, respectively (the last three quantities are all computed in the $\overline{\rm MS}$ scheme). These four "nuisance parameters" are the most relevant ones for accurately predicting the SUSY spectrum and its observable signature. In our analysis we thus consider an 8-dimensional parameter space spanned by the above four SM and the four CMSSM parameters.

In general, the results of a Bayesian analysis are expressed in terms of a posterior probability distribution (or more briefly, "a posterior"). By virtue of Bayes' theorem, the posterior is the product of the prior and the likelihood. The prior expresses the state of knowledge about the parameters before seeing the data, while the likelihood encodes the information coming from the observations (for further details on the Bayesian framework, see e.g. [9]). If the constraining power of the data is strong enough, then the posterior is effectively dominated by the likelihood and the prior distribution becomes irrelevant. However, if the observations are not sufficiently constraining, the posterior will retain a prior dependence. Therefore it is important to check to which extent the results based on the posterior pdf show a prior dependency. There are reasons to believe that for the CMSSM present data are not sufficiently powerful to completely override the prior, see [10] for a detailed study of this issue.

In our analysis we assume flat priors on both SM and CMSSM parameters over wide ranges of their values, encompassing the focus point region [8]. However, below we will comment on how our result change when one employs a flat prior in $\log_{10} m_{1/2}$ and $\log_{10} m_0$ instead (which we call in the following "the log prior" for brevity). The reason for this alternative choice of prior is that they are distinctively different. In particular, the log prior gives equal *a priori* weights to all decades for the parameters. So the log prior expands the low-mass region and allows a much more refined scan in the parameter space region where finely tuned points can give a good fit to the data (see [10] for details). Other choices of priors are possible and indeed physically motivated, and will be considered in future work. A recent discussion of some alternative prior choices in the CMSSM (motivated by considerations of naturalness and fine tuning) can be found in Ref. [11].

At every point in parameter space, we compute a number of observable quantities, and compare their values with the observational data listed in Ref. [6],[1] where also a detailed description of our procedure is given. We include all relevant collider limits, including direct limits on Higgs and superpartner masses, rare processes $\mathrm{BR}(\bar{B}\to X_s\gamma)$, $\mathrm{BR}(\bar{B}_s\to\mu^+\mu^-)$ and recently measured B_s mixing, ΔM_{B_s}, electroweak precision data (m_W and $\sin^2\theta_{\rm eff}$) and the relic abundance of the lightest neutralino $\Omega_\chi h^2$ assumed to be the cold DM in the Universe. We then use our MCMC algorithm [12] to produce, for a given model of DM distribution in the Galactic halo, probability distribution maps in parameter space and various observables, including ID ones which are computed with the help of DarkSusy [13]. As we have emphasized in Ref. [6], current constraints, especially from $b\to s\gamma$ favor the focus point region of large $m_0 \gtrsim 1$ TeV and not so large $m_{1/2} \lesssim 1.5$ TeV (with $m_{1/2} \lesssim 2.5 m_0$).

Table 1
Parameters for some popular halo profiles: a spherically symmetric modified isothermal model [15], the Navarro, Frenk and White (NFW) model [16] and the Moore et al. (Moore) model [17]. Everywhere $r_0 = 8.0$ kpc except for the isothermal case, where $r_0 = 8.5$ kpc. In the NFW and Moore et al. models the effect of adiabatic compression due to baryons (marked with an additional + ac), is included. See also Ref. [18].

Halo model	a (kpc)	α	β	γ	$\bar{J}(10^{-3}\mathrm{sr})$	$\bar{J}(10^{-5}\mathrm{sr})$
isothermal cored	3.5	2	2	0	30.35	30.40
NFW	20.0	1	3	1	1.21×10^3	1.26×10^4
NFW + ac	20.0	0.8	2.7	1.45	1.25×10^5	1.02×10^7
Moore	28.0	1.5	3	1.5	1.05×10^5	9.68×10^6
Moore + ac	28.0	0.8	2.7	1.65	1.59×10^6	3.12×10^8

3. Gamma-ray flux from the Galactic center

The differential diffuse γ-ray flux arriving from a direction at an angle ψ from the GC is given by [2]

$$\frac{d\Phi_\gamma}{dE_\gamma}(E_\gamma,\psi) = \sum_i \frac{\sigma_i v}{8\pi m_\chi^2}\frac{dN_\gamma^i}{dE_\gamma}\int_{\rm l.o.s.} dl\,\rho_\chi^2\big(r(l,\psi)\big), \tag{1}$$

where $\sigma_i v$ is a product of the WIMP pair-annihilation cross section into a final state i times the pair's relative velocity and dN_γ^i/dE_γ is the differential γ-ray spectrum (including a branching ratio into photons) following from the state i. Here we consider contributions from the continuum (as opposed to photon lines coming from one loop direct neutralino annihilation into $\gamma\gamma$ and γZ), resulting from cascade decays of all kinematically allowed final state SM fermions and combinations of gauge and Higgs bosons. The integral is taken along the line of sight (l.o.s.) from the detector. It is convenient to separate factors depending on particle physics and on halo properties by introducing the dimensionless quantity $J(\psi) \equiv (1/8.5\ \mathrm{kpc})(0.3\ \mathrm{GeV/cm^3})^2 \int_{\rm l.o.s.} dl\,\rho_\chi^2(r(l,\psi))$ [14]. The flux is further averaged over the solid angle $\Delta\Omega$ representing the acceptance angle of the detector, and one defines the quantity $\bar{J}(\Delta\Omega) = (1/\Delta\Omega)\int_{\Delta\Omega} J(\psi)\,d\Omega$.

Clearly, one of the crucial ingredients is the radial dependence of the WIMP density $\rho_\chi(r)$. Some popular profiles can be parameterized by [2]

$$\rho_\chi(r) = \rho_0 \frac{(r/r_0)^{-\gamma}}{[1+(r/a)^\alpha]^{\frac{\beta-\gamma}{\alpha}}}\big[1+(r_0/a)^\alpha\big]^{\frac{\beta-\gamma}{\alpha}}, \tag{2}$$

where the halo WIMP density has been normalized to its local value, assumed to be $\rho_0 = 0.3\ \mathrm{GeV/cm^3}$. Table 1 gives the values of the parameters: a, α, β, γ and r_0 for some common choices. Here we consider the line-of-sight (l.o.s.) integration factor $\bar{J}$ in the direction of the GC, i.e., for $\psi = 0$. In the case of the cuspy profiles, in order to avoid a divergent behavior, we set a cutoff radius of $r_c = 10^{-5}$ kpc. The total γ-ray flux from the cone $\Delta\Omega$ centered

[1] We employ the WMAP 3-year relic abundance value assuming that neutralinos are the only dark matter component. Using the WMAP 5-year value instead would not change visibly our results.

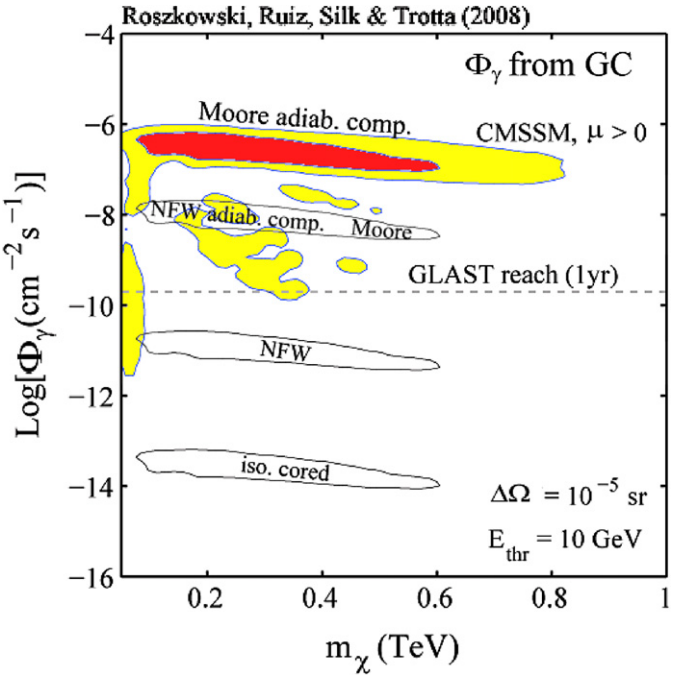

Fig. 1. The joint probability distribution for the γ-ray flux Φ_γ from the Galactic center vs the neutralino mass m_χ for some popular halo profile models, assuming flat priors, as explained in the text. The dark/red (light/yellow) region shows the predicted 68% (95%) probability ranges for the Moore profile with adiabatic compression (for other profiles we indicate only the limits of the 68% region). We also plot the expected 5-σ detection threshold (neglecting background) for energies above $E_\gamma = 10$ GeV for GLAST after 1 year of operation [21]. Notice that for GLAST to be able to detect the annihilation flux over the background one might require much larger fluxes than the sensitivity level plotted here [22]. (For interpretation of the references to color in this figure legend, the reader is referred to the web version of this Letter.)

on ψ and integrated over photon energy from an energy threshold $E_{\rm th}$, is then given by

$$\Phi_\gamma(\Delta\Omega) = \int_{E_{\rm th}}^{m_\chi} dE_\gamma\, d\Phi_\gamma/dE_\gamma(E_\gamma, \Delta\Omega). \tag{3}$$

With the launch of GLAST, which has angular resolution $\Delta\Omega \simeq 10^{-5}$ sr and sensitivity to fluxes larger than about 2×10^{-10} cm^{-2} s^{-1} for photon energies $E_\gamma \gtrsim 10$ GeV [21],[2] it is timely to investigate the global predictions of the CMSSM for a range of halo models.

Fig. 1 shows the joint probability distribution for the total flux Φ_γ from the GC above a threshold energy of 10 GeV versus m_χ, integrated over $\Delta\Omega = 10^{-5}$ sr. The spread of values reflects the marginalization over all the four CMSSM and four SM parameters, thus fully accounting for all substantial sources of uncertainty on the particle physics side. Firstly, as can be seen from the figure, the 2-dimensional joint 68% probability range of m_χ lies between about 80 GeV and about 600 GeV. Secondly, for a given halo profile, and assuming flat priors in CMSSM parameters, we find that the 68% probability range of Φ_γ is confined to lie within about one order of magnitude. On the other hand, the spread of the 95% probability range is much larger and at lower m_χ can extend over four or even five orders of magnitude.

In order to examine the low mass region in more detail, we have redone our analysis for the log prior choice introduced above. As $m_{1/2}$ and m_0 are the primary CMSSM parameters determining mass spectra of the neutralino, the other superpartners and the Higgs bosons, the log prior allows one to examine the low mass region in more detail, in particular by "expanding" the volume of the region 100 GeV $\lesssim m_{1/2}$, $m_0 \lesssim 1$ TeV. As we discuss below, the flat prior appears to produce an optimistic scenario as far as indirect detection signatures are concerned, while the log prior can give lower values of the fluxes and hence it leads to more pessimistic prospects for indirect detection. Ways of mediating between the two scenarios and to assess their relative plausibility will be explored in future work.

Since the log prior gives more "weight" to lower values of both $m_{1/2}$ and m_0, not surprisingly, we have found that it leads to a large widening of mostly the lower boundary of the 68% probability range at low m_χ, while not affecting the flux ranges at larger values of the neutralino mass. For example, the 68% probability range widens to nearly three decades and, in the case of the Moore profile with adiabatic compression, can be as low as 1.2×10^{-10} cm^{-2} s^{-1} at $m_\chi \sim 100$ GeV, but then it quickly raises and for $m_\chi \gtrsim 200$ GeV is not very different from the case of the flat prior. A more detailed discussion of the implications for CMSSM parameters of employing a log prior is given in Ref. [10].

For a given prior, choosing a different halo profile merely amounts to shifting the total flux by the ratio of the values of $\bar{J}$ given in Table 1. As expected, more cuspy profiles lead to higher predicted fluxes. We find that, in the CMSSM in the case of the Moore profile (with and without adiabatic compression) and the NFW profile with adiabatic compression, the continuum flux signal will be within the reach of GLAST, while for profiles with $\bar{J}(10^{-5}\ \mathrm{sr}) \lesssim 10^5$ it will not be detectable by GLAST. (We have checked that the case of $\mu < 0$ and flat priors gives qualitatively similar results.)

The differential γ-ray flux from DM annihilations is expected to exhibit a sharp drop-off in the energy spectrum as E_γ approaches m_χ. In Fig. 2 we plot 68% and 95% probability regions for the γ-ray differential flux for the NFW profile, averaged over a solid angle $\Delta\Omega = 10^{-3}$ sr (to allow a comparison with EGRET data), for the flat prior choice. Clearly, the current uncertainty on CMSSM parameters and hence on m_χ introduces a considerable spread in the predicted spectral shape of the signal. Additional uncertainty comes from the dependence on the priors. For example, for the log prior given above the 68% probability range of the differential photon range extends between 2.4×10^{-11} GeV cm^{-2} s^{-1} sr^{-1} and 6.7×10^{-7} GeV cm^{-2} s^{-1} sr^{-1}. Thus, even if a positive signal were detected by GLAST, it would be difficult to infer from it the mass of the WIMP, especially at its lower values below some 200 GeV, with any reasonable accuracy.

4. Positron flux from the Galactic halo

Positrons can be produced either in direct DM annihilation, or from decays and hadronization of other products (gauge and Higgs bosons, etc.), with the continuum spectrum from the latter usually dominating. Once produced, they propagate through the Galactic medium and their spectrum is distorted due to synchrotron radiation and inverse Compton scattering at large energies, bremsstrahlung and ionization at lower energies. The effects of positron propagation are computed following a standard procedure described in [24,25], by solving numerically the diffusion-loss equation for the number density of positrons per unit energy $dn_{e^+}/d\varepsilon$. The diffusion coefficient is parameterized as $K(\varepsilon) = K_0(3^\alpha + \varepsilon^\alpha)$, with $K_0 = 5.8 \times 10^{27}$ cm^2 s^{-1}, $\alpha = 0.6$ and $\varepsilon = E_{e^+}/(1\ \mathrm{GeV})$, mimicking re-acceleration effects. The energy loss rate is given by $b(\varepsilon) = \tau_E \varepsilon^2$, with $\tau_E = 10^{-16}$ s^{-1}, and we describe the diffusion zone (i.e., the Galaxy) as an infinite slab of height $L = 4$ kpc, with free escape boundary conditions. Changes in the above positron propagation model, especially $K(\varepsilon)$ (see e.g.

[2] Resolution and sensitivity in the range 30 MeV $\lesssim E_\gamma \lesssim$ 10 GeV are energy-dependent and would require a more careful analysis.

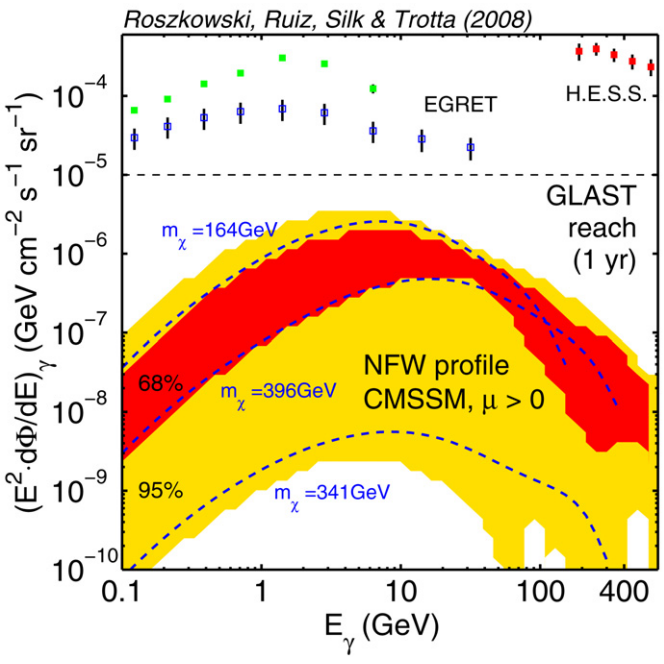

Fig. 2. Predicted γ-ray differential energy flux averaged over a solid angle $\Delta\Omega = 10^{-3}$ sr and fully accounting for current uncertainty in the CMSSM parameters, assuming flat priors. The 68% and 95% regions are for the NFW profile, all other cases can be obtained by rescaling them by the factors $\bar{J}$ given in Table 1. Predictions appropriate for GLAST resolution ($\Delta\Omega = 10^{-5}$ sr) are obtained by dividing by 1.21×10^3 and multiplying by the desired value of $\bar{J}(10^{-5}$ sr). We plot the expected GLAST 8σ detection threshold (horizontal black/dashed line [21]). The three blue, dashed curves show sample spectra (for the values of m_χ specified in the figure) from our statistical scan. For comparison we plot EGRET diffuse data towards the GC (green squares [19]), EGRET's point-source subtracted flux (blue empty squares [20]) and H.E.S.S. (2004) data [23] (red squares) with 2σ error bars. (For interpretation of the references to color in this figure legend, the reader is referred to the web version of this Letter.)

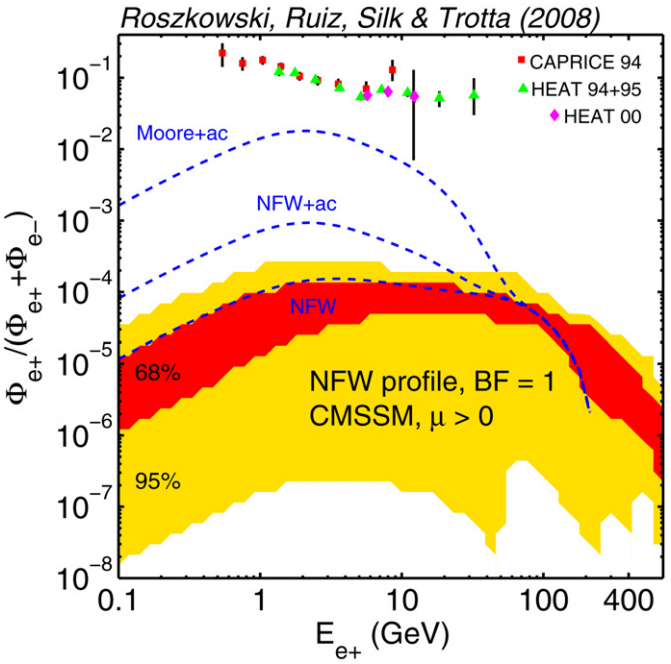

Fig. 3. Predicted positron flux fraction in the CMSSM. The 68% (dark/red) and 95% (light/yellow) regions are for an NFW profile with a boost factor BF = 1 and a specific choice of propagation model. We also show for comparison some of the current data. To illustrate the dependency of the spectral shape at low energies on the halo model, we plot the spectrum for the same choice of CMSSM parameters (with $m_\chi = 229$ GeV) for three different halo models as indicated. In absence of a large boost factor, the signal appears too small to be detected by PAMELA. (For interpretation of the references to color in this figure legend, the reader is referred to the web version of this Letter.)

[25,26]), can potentially lead to variations by a factor of 5 to 10 in the spectral shape at low positron energy, $E_{e^+} \lesssim 20$ GeV [27]. In this energy region the flux dependence on the halo profile is also substantial and, for the models in Table 1, the flux can change by up to a few orders of magnitude (compare blue/dashed lines in Fig. 3), since positrons from further away loose energy due to propagation. Most high-energy positrons, on the other hand, originate from the local neighbourhood the size of a few kpc s [25, 29], and their flux is less dependent of the halo and propagation dynamics. The flux can, however, be considerably enhanced by the presence of local DM clumps that survive merging processes and tidal stripping [28], an effect that is usually parameterized by a boost factor (BF), which can be of order 10. Recent studies have begun investigating the clumpiness dependence of the spectrum in more detail [29,30]. Finally, in order to reduce the impact of solar winds and magnetosphere effects on the model's predictions, it is useful to consider the positron fraction, defined as $\Phi_{e^+}/(\Phi_{e^+} + \Phi_{e^-})$, where Φ_{e^+} is the positron differential flux from WIMP annihilation, while Φ_{e^-} is the background electron flux. For background e^- and e^+ fluxes we follow the parametrization adopted in Ref. [25] from Ref. [26].

In Fig. 3 we show the predicted positron flux fraction in the CMSSM (for flat priors) for the NFW profile and a boost factor BF = 1, alongside a compilation of observations, most notably from HEAT. Again, the uncertainty in the spectral shape is one of the main results of our analysis, which accounts for the current uncertainties regarding the CMSSM parameters. The 95% probability region peaks in the range 1 GeV $\lesssim E_{e^+} \lesssim$ 10 GeV, roughly in the region of the apparent HEAT positron excess, but the strength of the signal is insufficient for it to be detectable by PAMELA in the absence of a large boost factor [31]. On the other hand, in that energy range the signal would be enhanced by more than one (two) order(s) of magnitude for a more cuspy profile such as the NFW (Moore) profile with adiabatic compression, as indicated in Fig. 3 for a sample spectrum corresponding to $m_\chi = 229$ GeV. This is because in the case of more cuspy profiles more high-energy electrons coming from the GC are scattered to lower energies. For the case of the log prior on $m_{1/2}$ and m_0 we again find a significant decrease of the lower boundary of the 68% range. For example, for the NFW profile with BF = 1 the ratio in Fig. 3 can be as low as 3.8×10^{-9}.

We conclude that, for not exceedingly cuspy halo models, PAMELA is unlikely to be sensitive to positron fluxes in the CMSSM, since for the NFW profile the signal is more than two order of magnitude smaller than the background. This result would qualitatively hold even when taking into account the considerable uncertainties coming from the boost factor due to local clumps and changes in the positrons propagation model, each of which can potentially change the spectrum by up to a factor of 10.

5. Summary

In the framework of the Constrained MSSM, we have performed a Bayesian analysis of prospects for indirect dark matter detection via a diffuse γ-ray signal or a positron flux from the Galactic center. This has allowed us to provide a statistically rigorous assessment of the uncertainty from the particle physics side of the problem.

We found that the prospects for GLAST to detect a diffuse γ-ray signal from the Galactic center depend primarily on the cuspiness of the DM profile at small radii. For the choice of flat priors in the CMSSM parameters, the NFW model appears to be a borderline

case, while a more cuspy halo would guarantee a signal for a 68% range of the CMSSM parameter space, except near the bottom end of the neutralino mass around 100 GeV, below the 68% probability range of m_χ. In the low mass region the sensitivity to the choice of priors remains however substantial. Adopting a log prior on $m_{1/2}$ and m_0 leads to a significant decreasing of the lower boundary of the 68% probability range of the γ-ray flux towards lower values at low $m_\chi \lesssim 200$ GeV, but at larger m_χ gives similar results as with flat priors.

On the other hand, a positron flux is unlikely to be detectable by PAMELA for both choices of priors, unless it is strongly enhanced by a nearby clump with a boost factor of at least of order ten. The latter conclusion is valid for a specific (although well motivated) choice of propagation model parameters. Assumptions regarding propagation parameters could however be easily relaxed in our framework. It would be straightforward to extend our treatment to include propagation model parameters as nuisance parameters and marginalize over them, as well. It is expected that such a procedure would increase the present, very substantial uncertainty as to the spectral shape, which we have shown is a consequence of the current lack of knowledge as to the preferred regions of the CMSSM parameters. Finally, it would also be interesting to repeat this analysis in a more general phenomenological SUSY model than the Constrained MSSM. While a richer phenomenology might help in explaining future signals should they be detected, it is also clear that a larger number of free parameters on the particle physics side will add to the difficulty of reliably predicting the shape and strength of both the γ-ray and the positron spectra.

Acknowledgements

We thank G. Bertone, I. Moskalenko and A. Strong for useful comments. R.R.d.A. is supported by the program “Juan de la Cierva” of the Ministerio de Educación y Ciencia of Spain. R.T. is supported by the Royal Astronomical Society and St Anne’s College, Oxford. We acknowledge partial support from ENTApP, part of ILIAS, and UniverseNet.

References

[1] See, e.g., G. Jungman, M. Kamionkowski, K. Griest, Phys. Rep. 267 (1996) 195; C. Muñoz, Int. J. Mod. Phys. A 19 (2004) 3093, hep-ph/0309346.
[2] G. Bertone, D. Hooper, J. Silk, Phys. Rep. 405 (2005) 279, hep-ph/0404175.
[3] G.L. Kane, C.F. Kolda, L. Roszkowski, J.D. Wells, Phys. Rev. D 49 (1994) 6173, hep-ph/9312272.
[4] See, e.g., H.P. Nilles, Phys. Rep. 110 (1984) 1.
[5] R. Ruiz de Austri, R. Trotta, L. Roszkowski, JHEP 0605 (2006) 002, hep-ph/0602028;
L. Roszkowski, R. Ruiz de Austri, R. Trotta, JHEP 0704 (2007) 084, hep-ph/0611173.
[6] L. Roszkowski, R. Ruiz de Austri, R. Trotta, JHEP 0707 (2007) 075, arXiv: 0705.2012.
[7] B.C. Allanach, C.G. Lester, Phys. Rev. D 73 (2006) 015013, hep-ph/0507283;
B.C. Allanach, C.G. Lester, A.M. Weber, JHEP 0612 (2006) 065, hep-ph/0609295.
[8] K.L. Chan, U. Chattopadhyay, P. Nath, Phys. Rev. D 58 (1998) 096004, hep-ph/9710473;
J.L. Feng, K.T. Matchev, T. Moroi, Phys. Rev. Lett. 84 (2000) 2322, hep-ph/9908309;
J.L. Feng, K.T. Matchev, T. Moroi, Phys. Rev. D 61 (2000) 075005, hep-ph/9909334.
[9] R. Trotta, Contemp. Phys. 49 (2) (2008) 71, arXiv: 0803.4089.
[10] R. Trotta, et al., arXiv: 0809.3792.
[11] B.C. Allanach, Phys. Lett. B 635 (2006) 123, hep-ph/0601089.
[12] The code is available from http://www.superbayes.org.
[13] P. Gondolo, et al., JCAP 0407 (2004) 008, astro-ph/0406204, http://www.physto.se/edsjo/darksusy/.
[14] L. Bergström, et al., Astropart. Phys. 9 (1998) 137, astro-ph/9712318.
[15] J. Binney, S. Tremaine, Galactic Dynamics, Princeton Univ. Press, Princeton, NJ, 1987.
[16] J.F. Navarro, C.S. Frenk, S.D.M. White, Astrophys. J. 462 (1996) 563, astro-ph/9508025;
J.F. Navarro, C.S. Frenk, S.D.M. White, Astrophys. J. 490 (1997) 493.
[17] B. Moore, et al., Astrophys. J. 524 (1999) 19.
[18] Y. Mambrini, C. Muñoz, E. Nezri, F. Prada, JCAP 0601 (2006) 010, hep-ph/0506204.
[19] H.A. Mayer-Hasselwander, et al., Astron. Astrophys. 335 (1998) 161;
As tabulated in: A. Cesarini, et al., Astropart. Phys. 21 (2004) 267, astro-ph/0305075.
[20] A.W. Strong, et al., Annu. Rev. Nucl. Part. Sci. 57 (2007) 285.
[21] See: http://tinyurl.com/yp6g5w (as of December 2007).
[22] G. Bertone, et al., astro-ph/0612387.
[23] F.A. Aharonian, et al., Phys. Rev. Lett. 97 (2006) 221102;
F.A. Aharonian, et al., Phys. Rev. Lett. 97 (2006) 249901, Erratum.
[24] J. Edsjö, M. Schelke, P. Ullio, JCAP 0409 (2004) 004, astro-ph/0405414.
[25] E.A. Baltz, J. Edsjö, Phys. Rev. D 59 (1999) 023511, astro-ph/9808243.
[26] I.V. Moskalenko, A.W. Strong, Astrophys. J. 493 (1998) 694, astro-ph/9710124;
I.V. Moskalenko, et al., arXiv: 0704.1328 [astro-ph].
[27] D. Hooper, J. Silk, Phys. Rev. D 71 (2005) 083503, hep-ph/0409104.
[28] J. Diemand, et al., Astrophys. J. 657 (2007) 262;
J. Diemand, et al., Nature 433 (2005) 389.
[29] J. Lavalle, J. Pochon, P. Salati, R. Taillet, astro-ph/0603796.
[30] See, e.g., D.T. Cumberbatch, J. Silk, Mon. Not. R. Astron. Soc. 374 (2007) 455, astro-ph/0602320;
Q. Yuan, X.J. Bi, astro-ph/0611872.
[31] Y. Mambrini, C. Muñoz, E. Nezri, JCAP 0612 (2006) 003, hep-ph/0607266.